A Glaciological Perspective on Heinrich Events

Garry K. C. Clarke and Shawn J. Marshall

Department of Earth and Ocean Sciences, University of British Columbia, Vancouver, Canada

Claude Hillaire-Marcel, Guy Bilodeau, and Christine Veiga-Pires

GEOTOP, Université du Québec à Montréal, Montréal, Québec, Canada

Heinrich events, the massive episodic disgorgement of sediment-laden ice from the Laurentide Ice Sheet to the North Atlantic Ocean, are a puzzling instability of the Ice-Age climate system. Although there is broad agreement on the defining characteristics of Heinrich events, the glaciological mechanisms remain controversial. Paleoceanographic records show that Heinrich events tend to occur at the culmination of a cooling cycle, termed the Bond cycle, and this has invited the interpretation that the events are a fast response of the Laurentide Ice Sheet to external atmospheric changes. A vexing issue for glaciologists is how a fast and timely response to an external forcing can possibly be reconciled with the known physics of glaciers and ice sheets. Fast changes in glacier behavior can only occur if some flow instability is excited. Thus glaciologists tend to favor the idea that the climate change occurring at the culmination of a Bond cycle is an atmospheric response to ice sheet instability. However, a free-running cyclic flow instability, such as that exhibited by surging glaciers, could not satisfy the timing requirements. Using computer modeling we explore ways to resolve these conflicts.

INTRODUCTION

The record of ice-rafted sedimentation in the North Atlantic ocean attests to the growth and decay of the Laurentide and Fennoscandian ice sheets during the last glacial cycle [*Ruddiman,* 1977]. A surprising feature of the marine sedimentary record is the evidence for synchronous and areally-extensive sedimentation events [*Heinrich,* 1988]. The provenance of these ice-rafted sediments can be traced to the Hudson Bay region of Canada [*Gwiazda et al.,* 1993a,b] and the accepted interpretation is that "Heinrich events" are associated with massive episodic disgorgement of sediment-laden icebergs from the Laurentide Ice Sheet [*Broecker et al.,* 1992]. An excellent recent review has been published by *Andrews* [1998].

Different scientific communities view Heinrich events from different perspectives—indeed from within different belief systems. To many glaciologists, Heinrich events fulfill the expectation that known glacier-scale flow instabilities are also expressed at the scale of ice streams and ice sheets. For several decades, glacial geologists have found this assumption useful [e.g., *Wright,* 1973; *Clayton, et al.,* 1985], although this hardly constitutes an observational proof. Among the important

Mechanisms of Global Climate Change at Millennial Time Scales
Geophysical Monograph 112

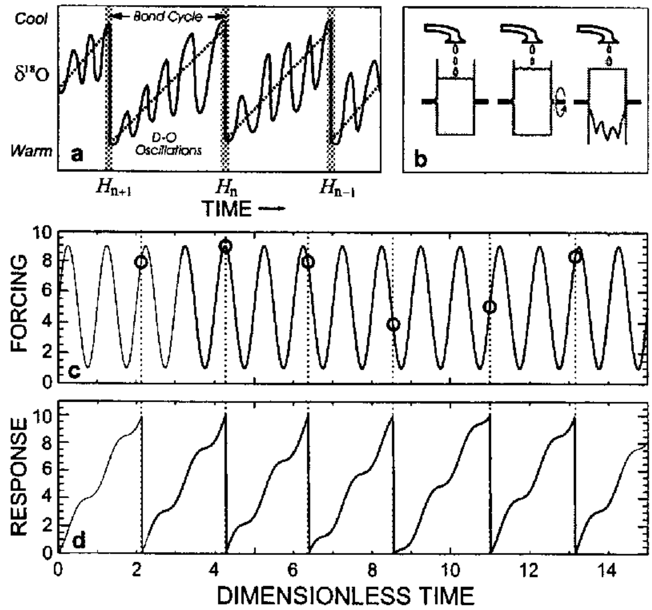

Figure 1. (a) Heinrich events bracket the Bond cycle. At the start of a Bond cycle climate is warm and at the end it is cold. Superimposed on this trend are millenial-scale climate oscillations known as Dansgaard-Oeschger oscillations. (b) MacAyeal's simple binge/purge oscillator is an example of a free-running oscillator. The timing of purge events is not synchronized with the external forcing. (c) Input forcing to a simple binge-purge simulation model. The forcing is water flux into the tipping bucket. A sinusoidal variation in forcing is assumed. (d) Response of simple binge-purge simulation model. The response is taken to be the water level in the tipping bucket. Purge events correspond to instantaneous drops in water level. Note that timing of purge events is independent of whether the filling rate is increasing or decreasing with time.

glaciological issues raised by Heinrich events, the following seem central:

(1) What was the order of events and what were the cause–effect relationships between continental ice dynamics and other components of the global climate system?

(2) Accepting that Heinrich events are evidence for large-scale flow instability of continental ice sheets, exactly what was the Laurentide Ice Sheet doing during Heinrich events? Which of several possible instability mechanisms were involved? How much ice was transferred from land to oceans?

(3) Can a physically consistent narrative be developed that does not violate present understanding of ice stream and ice sheet physics?

What follows is an overview of the glaciological issues that must be confronted, a commentary on inadmissible or unlikely possibilities, and an attempt to test some of these ideas using computer models.

ORDER OF EVENTS AND ISSUES OF TIMING

The marine and ice core paleoclimatic records agree on the principal features of Heinrich events and their relationship to other climate oscillations [*Bond et al.,* 1992, 1993; *Broecker,* 1994] and expose the problem of timing. Figure 1a sketches several Bond cycles; these are long-term cooling trends that are terminated by Heinrich events and upon which Dansgaard-Oeschger oscillations are superimposed. The coincidence of the onset of a Heinrich event with a pronounced climate switch has invited conflicting interpretations.

MacAyeal [1993a,b] has led the scientific attack by glaciologists and his "simple kitchen-built binge/purge oscillator" provides a good starting point for discussion of timing issues. Suppose the tipping bucket illustrated in Figure 1b is subjected to a sinusoidally-varying input flux (Figure 1c). Water level in the bucket rises at a variable rate until a critical threshold is reached and the tipping instability is triggered (Figure 1d). The instant at which the unstable response occurs is not synchronized with the forcing cycle (alignment of Figures 1c and 1d is indicated by vertical time lines; circle annotations on Figure 1c mark individual purge events). One cannot claim that the forcing and response are uncoupled but they lack the phase-lock that appears to characterize the ice-climate coupling associated with Heinrich events.

Anatomy of Heinrich Events

For complex phase-locked systems the question of distinguishing forcings from responses is murky. In principle the marine sedimentary record can resolve this difficulty but, for Heinrich events, coring sites distant from Hudson Strait [e.g., *Heinrich,* 1988] present a partial picture whereas those very close are cluttered by local effects [e.g., *Andrews et al.,* 1994]. The Orphan Knoll site (50°12.26N; 45°41.14W; 3448 m) appears to possess the advantages of proximity without the attendant disadvantages. A location map (Figure 2) shows the coring site and geographical features relevant to this paper. The site was first cored during a 1991 cruise of the CSS-Hudson (91-045-094, henceforth P-094; *Hillaire-Marcel et al.,* 1994), and again during the first North Atlantic campaign of the Marion-Dufresne II (MD-2024; *Stoner et al.,* 1998). The 11 m core P-094 spans isotopic stages 5a-1, whereas the 26 m core MD-2024 spans isotopic stages 5d-1. In spite of their large difference in length, both cores cover roughly the same time interval, the last Ice Age. Core MD-2024 yielded "stretched" records due to coring artifacts. Unfortunately, these also resulted in smoothing effects. Sedimentological, magnetic, and geochemical studies at 10 cm intervals (P-094) or 5 cm intervals (MD-2024), i.e., having a time resolution of a ~1000 yr and 250 yr, respectively, have already been published, with special attention to Heinrich layers [*Stoner et al.,* 1996]. In the present paper, we will refer to a new data set from P-094. It is based on samples collected at 1 cm intervals, i.e., with a theoretical resolution of 100 yr, but for the smoothing effect of bioturbations [see *Wu and Hillaire-Marcel,* 1994a]. The choice of core P-094, in preference to MD-2024, is based on the consideration that smoothing effects linked to coring artifacts, make MD-2024 records less reliable than those of P-094 for documenting the effects of short-term climate instability on sedimentation.

Figure 3 shows physical and sedimentological properties of the upper 6 m sequence in core P-094, a sequence that spans the time interval 0–45 kyr. We restrict the present study to the upper 6 m section of the core, because of its much better time control. The conversion of depth to calendar years is controlled by AMS ^{14}C age determinations (triangular annotations to the graph of $\delta^{18}O$ stratigraphy) and on high-resolution paleomagnetic correlations with other deep sea records [*Stoner et al.,* 1998; *Roberts et al.,* 1997]. Variations in $\delta^{18}O$ values in *Neogloboquadrina pachyderma* (s.) are taken as a proxy for salinity and, to a lesser extent, temperature changes in the upper water layer (i.e., a water layer between ~100 m and 500 m deep; see *Wu and Hillaire-Marcel* [1994b]). At the Orphan Knoll site, this proxy mainly indicates the dilution by ice meltwater of a water layer corresponding today to the upper Labrador Sea water mass [*Lucotte and Hillaire-Marcel,* 1994]. The ratio of anhysteretic remanent magnetization susceptibility K_{ARM} to low-frequency susceptibility K decreases with increasing magnetic grain size when the magnetic mineralogy is dominantly magnetite [*Stoner et al.,* 1996]. This indicator is taken as a proxy for the settling of suspended sediment produced by turbiditic flow down the Northwest Atlantic Mid-Oceanic Channel (NAMOC in Figure 2). The coarse fraction (>125 μm weight per cent) is viewed as an indicator of ice-rafted debris (IRD) [*Hillaire-Marcel et al.,* 1994a] as well as of coarse debris-flow sedimentation channeled by the NAMOC [e.g., *Hesse and Rakofsky,* 1992]. In the fast-deposited units, such as Heinrich layers, the weight per

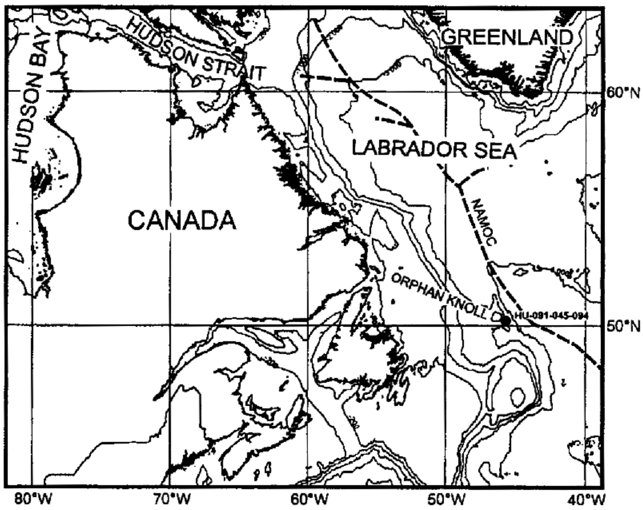

Figure 2. Map of Labrador Sea region of Eastern Canada showing bathymetric contours and the location the drilling site east of Orphan Knoll from which core HU-91-045-094P was recovered. The Northwest Atlantic Mid-Oceanic Channel (NAMOC) is indicated by a dashed line.

cent $CaCO_3$ is associated with silt-size suspended sediment transport and/or with overspilled turbidites from the NAMOC, rather than with ice-rafting. This material originates from glacial erosion of Paleozoic carbonates in Hudson Strait area [e.g., *Andrews et al.,* 1994]. The ratio $^{230}Th_0/^{232}Th$ (Figure 4) is an indicator of sedimentation rate. ($^{230}Th_0$ denotes the ^{230}Th activity corrected for radioactive decay since deposition, i.e., the ^{230}Th activity of the sediment when it settled. ^{232}Th labels terrigenous fluxes, whereas ^{230}Th includes a terrigenous fraction, a diagenetic fraction due to the decay of the diagenetically uptaken U in the sediment, and most importantly for this indicator, a fraction produced by the decay of U dissolved in the overlying water column and a fraction scavenged by the settling particles [see *Hillaire-Marcel et al.,* 1994b].)

Scrutiny of the $\delta^{18}O$ variations shown in Figure 3 reveals that all the Heinrich events started while the ocean state was cold and that onset of a Heinrich event is signalled by a sharp increase in K_{ARM}/K, indicating a rapid increase in sediment flow along NAMOC which guides submarine suspended sediment from Hudson Strait to the core site. Over the five Heinrich events, this increase tends to be well correlated with increases in coarse fraction and $CaCO_3$. The timing of maximum dilution by iceberg melting (indicated by local minima on the $\delta^{18}O$ plot and a second peak in coarse fraction

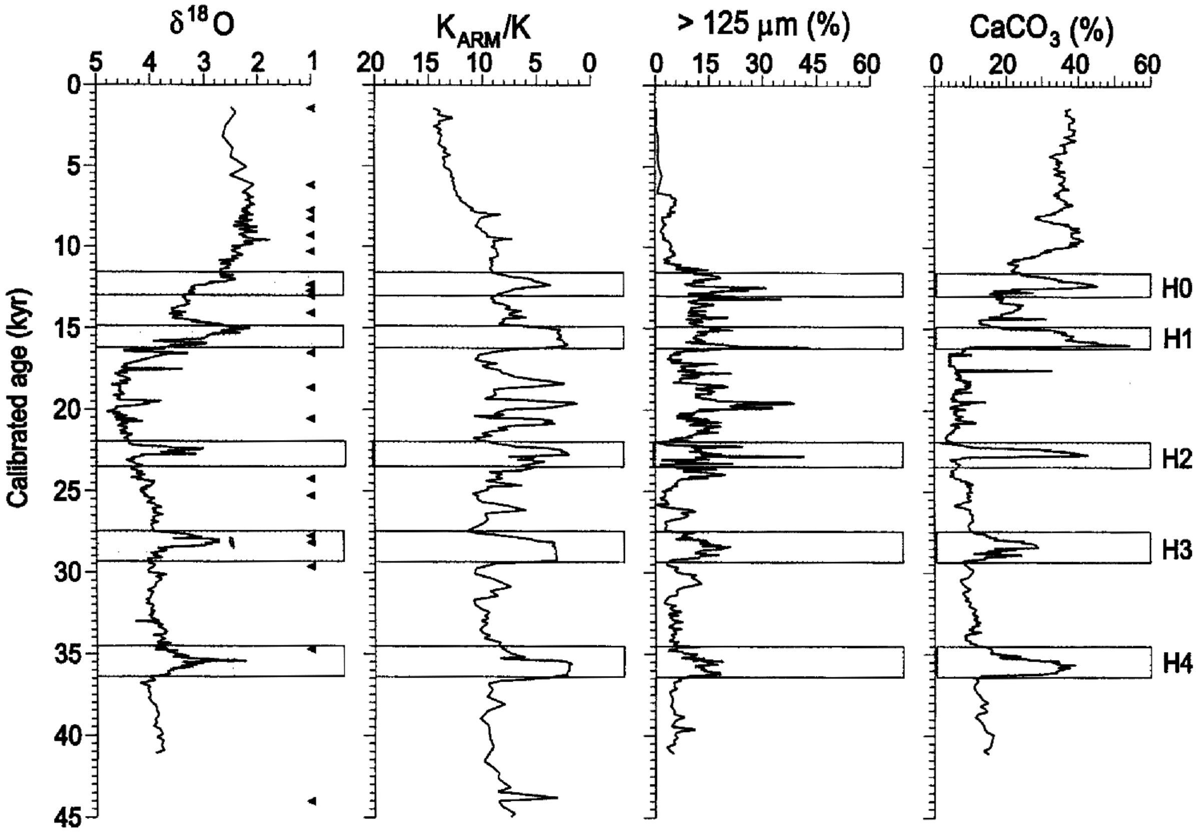

Figure 3. Properties of the studied sequence in core HU-91-045-094P. Heinrich events H0 to H4 are indicated. (K_{ARM}/K values are from *Stoner et al.* [1996].)

content) is delayed relative to these sedimentation signals. This interpretation is entirely based on analysis of the HU-91-045-094P core, which yields the most detailed available record of the composite nature of Heinrich layers.

Figure 4 provides a closer look at the H1 and H0 events and includes results of $^{230}Th_0/^{232}Th$ measurements from *Veiga-Pires and Hillaire-Marcel* [under revision] which help to document the relative changes in sedimentation rates during these two events. We shall use the calendar age axis as an aid to cross-referencing between the graphs but it is important to recognize that these values are subject to all the ambiguities associated with the interpolation of ages between precisely dated levels. Our references to calendar ages are intended to facilitate discussion of the sequence of events, not to fix their absolute timing or duration. At 16.4 kyr the $\delta^{18}O$ plot shows a cold peak immediately preceding the onset of H1. From 16.4 kyr–15.1 kyr there is a decreasing trend in $\delta^{18}O$ that is interpreted as a progressive isotopic lightening of near-surface waters by iceberg melt, 15.1 kyr corresponding to maximum dilution. The major peak in coarse fraction occurs at 16.2 kyr and is accompanied by a pronounced increase in K_{ARM}/K. The absence of a correspondingly strong local minimum in $\delta^{18}O$ suggests to us that this increase in coarse fraction deposition is not primarily an effect of enhanced IRD, because a larger flux of icebergs should result in diluted low $\delta^{18}O$ surface waters. Instead, we believe that the increase in coarse fraction is an indication of active debris-flows channeled along NAMOC, possibly signalling advancing ice and accompanying sediment disturbance in the Hudson Strait area. From 16.1 kyr–16.0 kyr there is a striking increase in $CaCO_3$ accompanied by a rapid increase in sedimentation rate (decrease in $^{230}Th_0/^{232}Th$). The $CaCO_3$ increase is not a result of IRD and the grain size is suggestive of glacial flour; this could be associated with suspended sediment released by the subglacial water system of an actively-flowing ice stream. The interval from 16.1 kyr–15.1 kyr is characterized by fast deposition (low $^{230}Th_0/^{232}Th$), predominantly of fine-grained $CaCO_3$. From 15.2 kyr–15.1 kyr

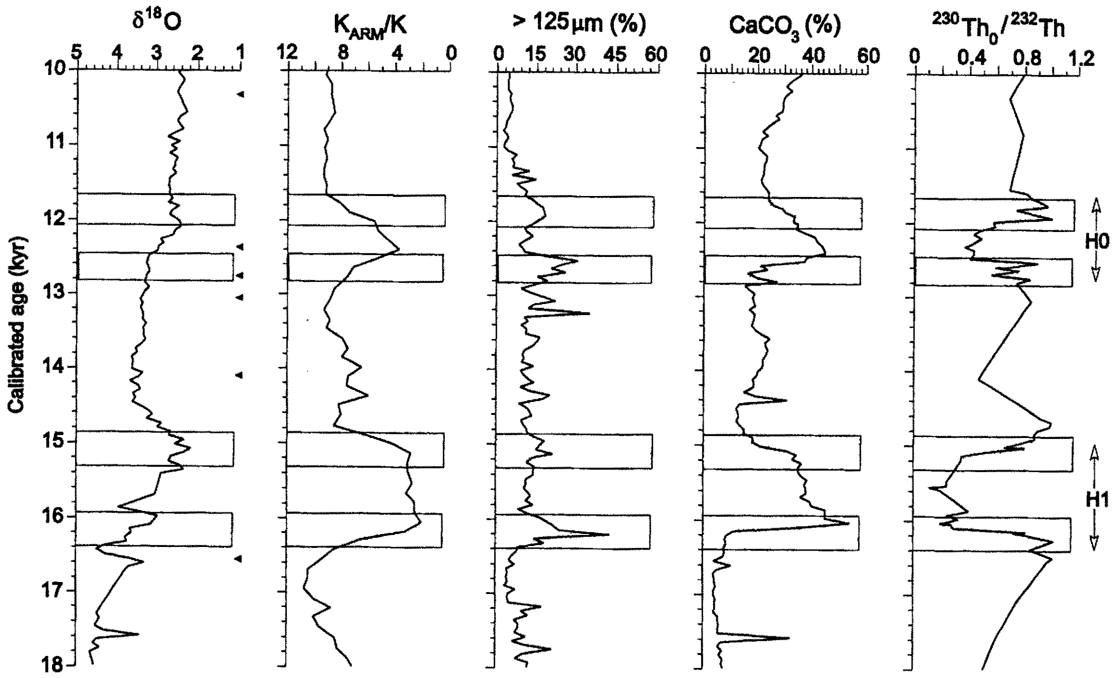

Figure 4. Details of H1 and H0 in core HU-91-045-094P. (K_{ARM}/K values are from *Stoner et al.* [1996] and $^{230}Th_0/^{232}Th$ values are from *Veiga-Pires and Hillaire-Marcel* [under revision].)

a minor peak in coarse fraction is very well correlated with the $\delta^{18}O$ minimum at maximum dilution. This is interpreted as the principal IRD peak for H1.

A similar close examination of H0 (Figure 4) leads to the following interpretation. Around 12.8 kyr the first indications of H0 appear as a progressive increase in coarse fraction (12.8 kyr–12.5 kyr) leading to a major coarse fraction peak at 12.5 kyr. This interval is followed by a rapid increase in fine-grained $CaCO_3$ beginning around 12.5 kyr and coinciding with a fast-deposition interval (12.5 kyr–12.0 kyr as indicated by $^{230}Th_0/^{232}Th$). Significantly, the $\delta^{18}O$ signal is unaffected by the initial major coarse fraction peak suggesting that sedimentation over the interval 12.8 kyr–12.5 kyr is associated with debris-flows along NAMOC and not with IRD, as also seen in the H1 layer. From 12.5 kyr–12.0 kyr there is a progressive decrease in $\delta^{18}O$ and maximum dilution occurs at 12.0 kyr, followed at 11.9 kyr by a minor peak in coarse fraction which we interpret as the IRD peak for H0.

In the near-field, both H1 and H0 reveal a two-part structure highlighted by their two coarse fraction peaks. This twin-peak structure is not a calculation artifact linked to the dilution of the total sediment by the fine-detrital carbonates. The two peaks remain clearly defined when coarse fraction contents are evaluated for $CaCO_3$-free sediment [*Veiga-Pires and Hillaire-Marcel,* under revision] and they constitute a typical feature of most Heinrich layers in the Orphan Knoll area. At this site, the first sedimentary signal of Heinrich events is associated with enhanced debris-flow deposition presumed to be linked to advancing ice in the vicinity of Hudson Strait, i.e., at the head of the principal NAMOC tributaries. The major IRD peak is delayed relative to the onset of these Heinrich events and is associated with maximum dilution by iceberg melting. Additional evidence for the involvement of two distinct depositional mechanisms for the coarse fraction peaks of Heinrich layers is provided by the fact that at least two of these layers show erosional surfaces at the very base of the bottom peak (notably H3 and H6; see *Hillaire-Marcel et al.* [1994a]). Furthermore, lithic fragment counts in the H1-H0 sequence, which we looked at in greater detail, indicate that the bottom coarse fraction peak has a proportion of carbonate debris typically exceeding 50%, likely due to their restricted source in the carbonate-rich area of Hudson Strait, whereas the top peak shows a substantially reduced proportion of such carbonate fragments (~20%) and more silicate grains, suggesting IRD by icebergs from more scattered sources. A modeling study of IRD during Heinrich events [Alley and MacAyeal, 1994] predicts a two-peak structure in IRD sedimentation but differs in detail from our interpretation. The essential point of difference is that in the modeling study the two peaks result from a single depositional mechanism whereas evidence from core HU-91-045-094P points to the sequential operation of two distinct mechanisms.

It is informative to consider the question: "How would the signals that are preserved in the Orphan Knoll core be transmitted to mid-Atlantic sites?" In particular, if the major coarse fraction peak at Orphan Knoll is indeed associated with turbiditic transport along NAMOC and not with IRD, then this signal would not be found in cores at sites distant from Hudson Strait. At these sites the paleoceanographic record of Heinrich events would be that of a progressive decrease in $\delta^{18}O$ culminating in an IRD episode.

PHYSICAL CONSTRAINTS ON SURFACE-TO-BED COUPLING

The Orphan Knoll data show no evidence of a premonitory climate forcing causing a cryospheric response. Most glaciologists favor the view that Heinrich events are not climate-triggered and computer models have been developed to demonstrate that Hudson Strait Ice Stream can plausibly behave as a free-running oscillator [*MacAyeal*, 1993a,b; *Marshall and Clarke*, 1997a,b]. The problem with this conclusion is that a free-running oscillator, such as the simple kitchen-built oscillator, would lack the phase-locking between climate state and ice volume that seems to be a feature of the ice–climate system before the onset of a Heinrich event. The occurrence of Heinrich events during the cold phase of a Dansgaard-Oeschger (D-O) oscillation needs explanation. One might suggest that, like Heinrich events, the D-O oscillations are a consequence of cryospheric forcing of climate but the marine sedimentary record leaves this question undecided [*Bond et al.,* 1997]. It appears that during the long onset period, ice–climate coupling is an expression of climate forcing of a cryospheric response. How this can be effected is a challenging question for glaciologists.

It is important to appreciate that the flow of glaciers and ice sheets is largely dictated by processes that are active at the glacier bed whereas atmospheric forcing operates at the upper surface. For any surface process to produce a flow response there must be transmission of this influence from the surface to the bed. The list of surface-to-bed couplings is short and several processes can be dismissed as untenable.

Extreme and rapid changes in surface temperature are propagated to the bed with substantial attenuation

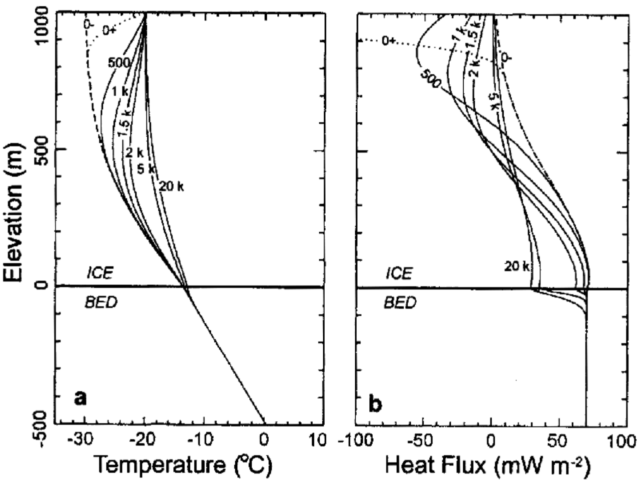

Figure 5. Response of a 1000 m thick ice slab to a 10°C increase in surface temperature. Ice rests upon bedrock. The ice–bed interface is taken as the elevation datum. The time slices are for 0^- (immediately before the temperature increase), 0^+ (immediately after), 500 yr, 1 kyr, 1.5 kyr, 2 kyr, 5 kyr, and 20 kyr. (a) Temperature as a function of elevation. (b) Upward heat flux as function of elevation.

and delay. For conductively-dominated heat transport the characteristic time constant for diffusion is $t_C = \rho_I c_I H_I^2/K_I$, where ρ_I is ice density, c_I is the specific heat capacity for ice, H_I is ice thickness, and K_I is the thermal conductivity of ice. For advectively-dominated heat transport the time constant is $t_A = H_I/b_I$ where b_I is the ice-equivalent surface accumulation rate. Taking $H_I = 1000\,\mathrm{m}$, $b_I = 0.25\,\mathrm{m\,yr^{-1}}$, and physical constants consistent with *Paterson* [1994] gives $t_C \sim 28\,\mathrm{kyr}$ and $t_A \sim 4\,\mathrm{kyr}$. Figure 5 presents simulation results that illustrate the combined effects of diffusion and advection in a 1000 m thick ice slab subjected to an instantaneous 10°C increase in surface temperature. Even after 2 kyr there is no appreciable increase in bottom temperature. All paths point to the same conclusion: surface temperature variations, regardless of how large they are and how rapidly they occur, cannot be effectively transmitted to the beds of ice streams and ice sheets.

Hydrological coupling, an alternative to thermal coupling, can be both fast and strong. If surface melting accompanies an increase in surface temperature and meltwater can percolate from the ice sheet surface to the bed, a fast flow response might be coupled to some surface forcing, for example an increase in surface temperature or a decrease in surface albedo (e.g., from dust deposition). Modern mountain glaciers demonstrate this coupling in the form of strong diurnal and seasonal cycles in flow rate. It is extremely unlikely that this is a significant process in modern continental ice sheets and it is unlikely that the Laurentide Ice Sheet behaved differently except during the late stages of its disintegration. As evidenced in Figure 5, summer meltwater would have to percolate through great thicknesses of extremely cold ice before a surface-to-bed coupling could be activated. Although hydrological coupling between the ice surface and the bed can occur rapidly and produce a large ice flow response, we do not consider this a likely possibility throughout most of the lifetime of the Laurentide Ice Sheet.

The transmission of stress from the surface of an ice sheet to its bed occurs virtually instantaneously. Any increase in surface loading, for example from increased accumulation rate, would produce an instantaneous mechanical response at the glacier bed. A problem with mechanical coupling between the surface and bed is that it is difficult to load the surface rapidly; a greatly increased surface accumulation rate cannot produce a rapid thickness increase. In summary, this form of surface-to-bed coupling is very strong, but it is difficult to justify a surface forcing of substantial amplitude. Nevertheless mechanical coupling is the only viable surface-to-bed coupling of those identified. We shall revisit this discussion in a subsequent section.

MECHANISMS OF FAST FLOW AND FLOW INSTABILITY

Ice creep is a slow but ubiquitous process. Fast flow, such as that associated with ice stream motion and the active state of surging glaciers, is caused by basal flow processes—sliding and deformation of subglacial sediment. The relative importance of these fast-flow processes remains controversial [*Alley*, 1989; *Kamb*, 1991; *Iverson et al.*, 1995] and is likely to vary both spatially and temporally. Whereas the creep process can operate in cold ice, sliding and bed deformation are only effective if the bed is at the ice melting temperature. Although this is a necessary condition for fast flow, it is by no means a sufficient condition. Fast flow is enabled by thermal conditions but activated by hydrological conditions. There are numerous examples of valley glaciers that are permanently at their melting temperature at the bed but which slide negligibly unless subglacial water pressure is high [e.g., *Iken and Bindschadler*, 1986]. Because the thermal and mechanical physics of glaciers is well known but the processes controlling subglacial hydrology, sliding, and bed deformation are comparatively poorly known, most current ice sheet models ignore hydrology entirely.

Ice Stream Surging

MacAyeal [1993a,b] was the first to use computer models to explore the possibility that Heinrich events are associated with episodic surging of Hudson Strait Ice Stream. His low-order model has similar physics to a thermal model developed to describe cyclic surging of Trapridge Glacier, Yukon Territory, Canada [*Clarke*, 1976] and shares the major shortcoming of that model—onset and termination of fast flow are exclusively controlled by thermal conditions at the bed. Field studies of Variegated Glacier, Alaska, during its 1982-83 surge [*Kamb et al.*, 1985; *Raymond*, 1987] demonstrate that surging is predominantly controlled by subglacial hydrological processes rather than thermal processes and that the cause of fast flow is elevated subglacial water pressure.

Generalized characteristics of a surge cycle for a glacier that, like Hudson Strait Ice Stream, discharges ice into the ocean are presented in Figure 6. Modern examples of such glaciers can be found in Svalbard [*Schytt*, 1969] and East Greenland [*Reeh et al.*, 1994] and it is apparent that individual behaviors will be influenced by factors such as water depth and bed geometry. At the onset of a surge, ice flow rate increases dramatically and the terminus advances (Figure 6a). As the advance proceeds, the calving rate increases (Figure 6b) and the ice stream thins. The stopping mechanism for ice stream surges is not known. For mountain glaciers it appears that the subglacial water system switches from an areally-distributed sheet-like configuration to a spatially-localized conduit configuration and this transformation leads to a rapid drop in subglacial water pressure [*Kamb et al.*, 1985]. A similar explanation might apply to ice streams but it is also possible that the combined effects of reduced ice thickness and surface slope eventually lead to a reduction in bottom stress and that the accompanying decrease in subglacial meltwater production terminates the surge (Figure 6c). Following the surge, the ice–bed contact might refreeze but this is not an essential feature of the surge mechanism.

Ice Shelf Breakup

The recent breakup of Larsen Ice Shelf in the Antarctic Peninsula [*Vaughn and Doake*, 1996; *Doake et al.*, 1998] reminds glaciologists that large iceberg fluxes are not necessarily associated with fast-flowing ice. In the case of ice shelf breakup, the ice flow rate need not vary markedly and the most conspicuous manifestation of breakup is upflow migration of the calving front. Figure

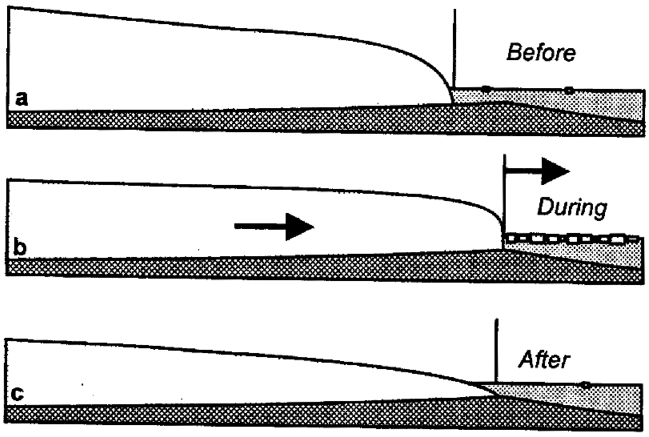

Figure 6. Ice stream surging mechanism. (a) Pre-surge state. (b) Active phase. (c) Post-surge state.

7 summarizes the sequence of events. Prior to breakup the shelf extends well beyond its grounding line (Figure 7a); lack of nourishment, or some other trigger, causes breakup to initiate (Figure 7b) and the calving front moves inland; breakup ceases when the shelf disappears (Figure 7c). *Hulbe* [1997] has successfully modeled this sequence of events.

Tidewater Instability

Like the ice shelf breakup mechanism, tidewater instability is associated with retreating, rather than advancing ice. The dramatic retreat of Columbia Glacier, Alaska, provides a well-documented modern example of this instability in operation [*Meier and Post,* 1987; *Meier et al.,* 1994; *Kamb et al.,* 1994]. Ice calving lies at the heart of this instability and, unfortunately, this process is poorly understood. Adopting ideas from *Reeh* [1968], *Brown et al.* [1983], and *Meier and Post* [1987], *Marshall et al.* [submitted] have expressed the calving discharge per unit width Q_c (in $\mathrm{m}^2\,\mathrm{yr}^{-1}$) as

$$Q_c = k_c H_W H_I \qquad (1)$$

where H_W is water depth, H_I is ice thickness, and k_c is a rate parameter which can include the effects of calving geometry, ice temperature, and longitudinal stress. The key feature of (1) and most empirical calving laws is that calving rate is proportional to water depth. This introduces the possibility of unstable behavior. If dH_W/ds (the downflow slope of the sea floor) is negative then water depth decreases as ice flows toward the calving margin. During advance of a tidewater glacier, ice volume is increasing. The further ice advances, the lower the water depth and, by (1), the lower the calving rate. Ice input exceeds output and thickness increases until the calving rate and inflow are in balance (Figure 8a). If ice supply then decreases, the calving rate would exceed the inflow and the calving margin would retreat from its stable position. In retreat, the system cannot produce a stable response. As the calving front recedes, water depth increases as does the calving rate (Figure 8b). This positive feedback continues until the calving front reaches a region where a new equilibrium can be established (Figure 8c).

For glaciers it is known that surging is a cyclic internal flow instability and external factors such as climate change have only a secondary influence on the cycle. In contrast, tidewater instability is ultimately a response to trends that affect glacier mass balance; thus this instability is the more amenable to a climate trigger. An alternative trigger, suggested by *Paterson* [1998], draws on *Alley's* [1991] suggestion that a tidewater retreat can be initiated by the advance of a tidewater glacier beyond its stable grounding position.

Other Possibilities

Although there are no modern examples, compound instabilities that involve combinations of the foregoing mechanisms cannot be ruled out. Possible examples include: (i) ice-shelf breakup triggering a surge, (ii) ice shelf breakup triggering a catastrophic tidewater retreat, and (iii) a surge advance followed by tidewater instability.

It has recently been suggested that Heinrich events are triggered by earthquakes that are induced by ice

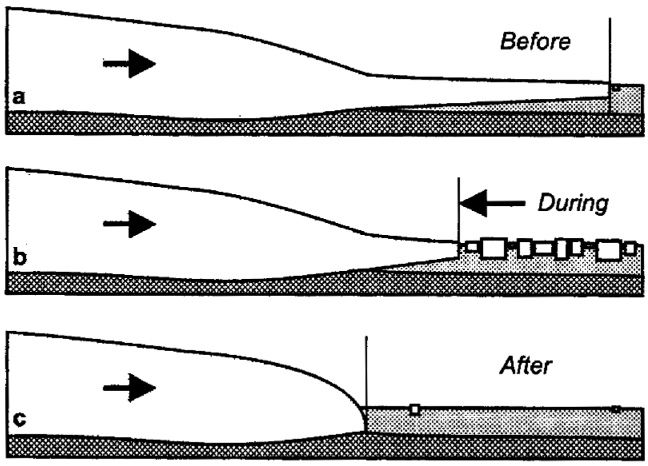

Figure 7. Ice shelf breakup mechanism. (a) Before onset of breakup instability. (b) During active breakup phase. (c) Post-breakup state.

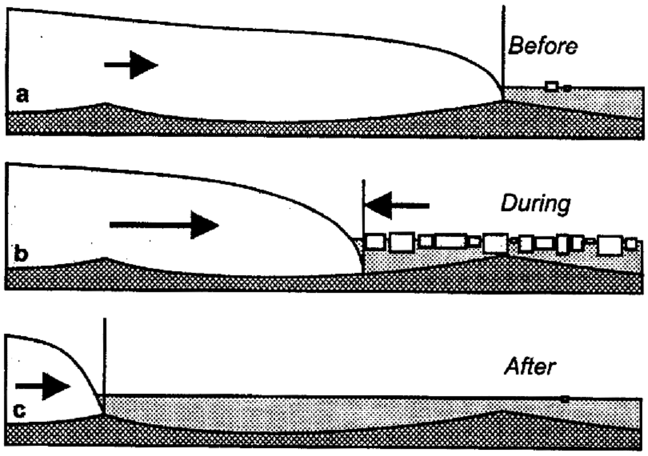

Figure 8. Tidewater instability mechanism. (a) Before onset of calving instability. (b) During catastrophic retreat. (c) Following termination of calving instability.

loading in the vicinity of Hudson Strait [*Hunt and Malin,* 1998]. Apart from the loose claim that Hudson Strait Ice Stream might behave as an "ice slide", the proposal has no basis in glacier physics and, indeed ignores the entire relevant literature on the subject. The ice slide hypothesis can be traced to *Saussure* [1779-96] and was superceded by the field studies of *Forbes* [1842]. The earthquake-advance theory is associated with *Tarr and Martin* [1914] who happened to be studying Alaskan glaciers shortly after the occurrence of a major earthquake. By an unremarkable coincidence one of Alaska's many surge-type glaciers was observed to be actively surging and this led to their plausible inference. *Post* [1965] formally tested the earthquake-advance theory and concluded that it was unsupported by observations. While wrong, *Tarr and Martin's* [1914] theory is at least sensible; Alaskan glaciers subjected to large earthquakes can receive an increased surface load contributed by earthquake-triggered avalanches. For Hudson Strait Ice Stream, avalanche loading is not a possibility and earthquake-triggered decoupling of the ice stream from its bed is completely inconsistent with modern understanding of ice stream dynamics.

Problems of sediment entrainment and retention

Another challenging problem associated with Heinrich events is to explain the vast quantities of sediment exported to the North Atlantic Ocean from the Hudson Bay region of Canada. Vast amounts of sediment imply vast amounts of ice [*Alley and MacAyeal,* 1994; *Dowdeswell et al.,* 1995]. This is not the end to the difficulty; even if large ice volumes are accepted, it seems necessary to invoke a highly-efficient sediment entrainment mechanism.

A further problem relating to sediment is explaining sediment retention. Entrainment processes operate most effectively near the ice–bed contact and the foreseeable result is accretion of a sub-horizontal layer of debris-rich ice. Bottom melting works against sediment entrainment and retention and, because fast flow processes are launched and sustained by geothermal and frictional meltwater production at the ice-bed contact, the requirements of fast ice flow and efficient sediment entrainment appear to conflict. The rate of bottom melting $\dot{m}$ (in $\mathrm{m\,yr^{-1}}$) is given by the expression

$$\dot{m} = \frac{1}{n_I \rho_I L} \left(q_F + q^- - q^+ \right) \tag{2}$$

where n_I is the volume fraction of ice, L is the latent heat of melting for ice, $q_F = v_S \tau_B$ is the heat flux generated by sliding friction (where v_S is the sliding rate and τ_B is the basal shear stress), $q^- = -K^-(\partial T/\partial z)^-$ is the heat flux immediately below the ice–bed contact, and $q^+ = -K^+(\partial T/\partial z)^+$ is the heat flux immediately above it. Heat flux q can be discontinuous across this boundary as can the thermal conductivity K and temperature gradient $\partial T/\partial z$; superscripts "+" and "−" respectively denote the regions immediately above and below the contact.

Ice that calves from the Laurentide Ice Sheet is subjected to melting by sea water. Melting rates depend on temperature and salinity [*Russell-Head,* 1980] and, for bergs that do not roll over, bottom-accreted sediment is the first casualty of melting. These considerations suggest that a substantial thickness of sediment-rich ice is required and that entrainment mechanisms that inject sediment beyond the ice–bed contact favor long-term sediment retention.

Figure 9 illustrates five known mechanisms for sediment entrainment. Thermal freeze-down (Figure 9a) is the classic mechanism [*Weertman,* 1961] and the mechanism associated with *MacAyeal's* [1993a,b] binge/purge model. A shortcoming of the freeze-down mechanism is that it requires downward migration of the freezing plane and, typically, this occurs very slowly beneath thick ice. If $Z(t)$ is the elevation of the freezing plane then

$$\frac{dZ}{dt} = \frac{1}{n_E \rho_I L} \left(q^- - q^+ \right) \tag{3}$$

where n_E is the porosity of unfrozen water-saturated bed material, and q^+ and q^- are as previously defined.

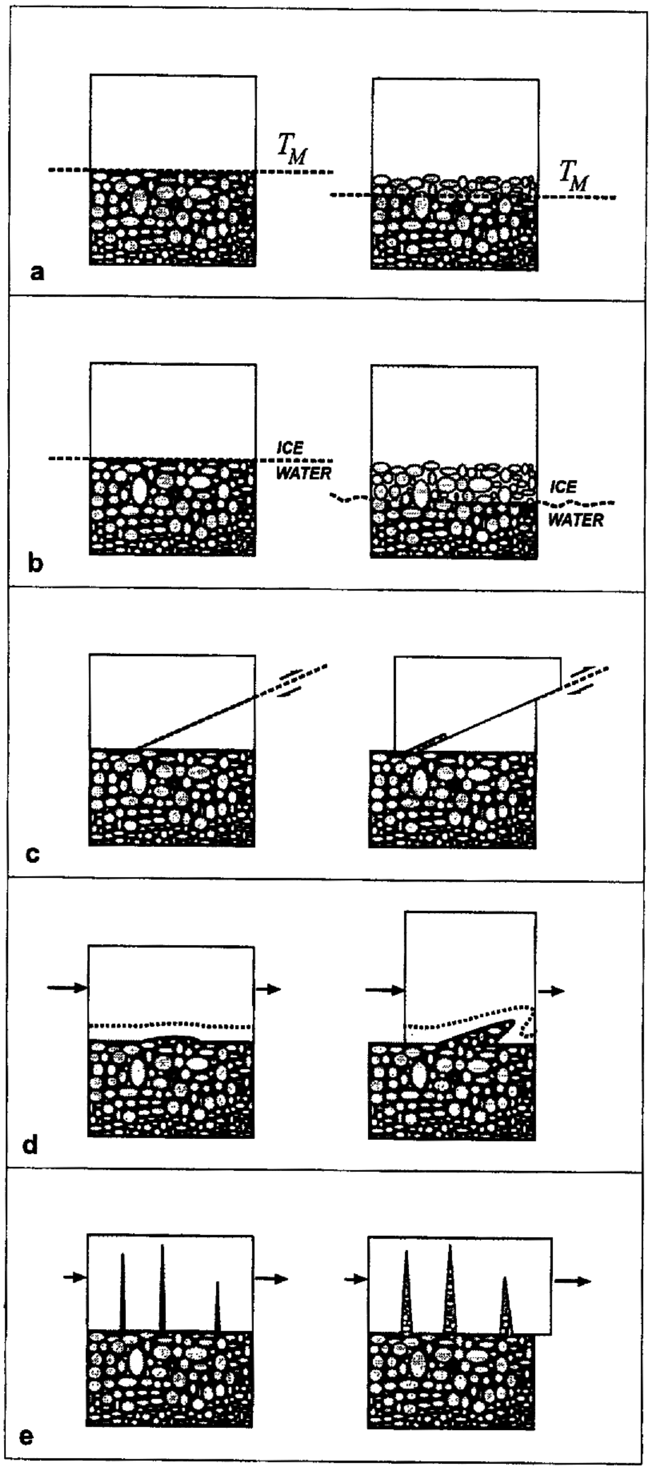

Figure 9. Sediment entrainment mechanisms. (a) Thermal freeze-down. (b) Regelation infiltration. (c) Thrusting. (d) Folding. (e) Bottom crevassing.

From Equation (3) it is evident that the large latent heat of fusion for water works against rapid motion of the freezing plane.

An entrainment process that is likely to be more effective than freeze-down is the process of regelation infiltration (Figure 9b) [*Iverson,* 1993; *Iverson and Semmens,* 1995]. According to the theory of *Phillip* [1980], ice at its melting temperature infiltrates underlying sediment at a rate

$$\frac{dZ}{dt} = -k(p_I - p_W) \tag{4}$$

where $p_I = \rho_I g H_I$ is the ice overburden pressure and p_W is the water pressure beneath the ice–bed contact. The rate factor k decreases as the thickness of ice-entrained sediment increases. The infiltration process underlying (4) is regelation; pressure melting occurs at the contact with a resisting clast and refreezing follows as the clast is passed. If subglacial water pressure is low, the process can proceed rapidly. Like the thermal freeze-down mechanism, there is a moving phase boundary but the migration rate is not controlled by macroscopic heat fluxes.

The entrainment processes of thrusting [*Clarke and Blake,* 1991], folding, and bottom crevassing [*Sharp,* 1985] are tectonic (Figures 9c–9e) and difficult to quantify. Tectonic processes share the attractive feature that sediment is stored at some distance from the ice–bed contact and this style of entrainment would delay the timing of sediment release by berg melting.

EVALUTION OF CANDIDATE MECHANISMS

The foregoing discussion sets the stage for an evaluation of the candidate instability mechanisms. Although each of the candidates, surging, ice shelf breakup, and tidewater instability, seems capable of explaining the large iceberg fluxes associated with Heinrich events, their sediment entrainment and sediment preservation characteristics differ.

Cyclic surging of mountain glaciers is associated with pronounced cyclic variations of stress [*Raymond et al.,* 1987] and subglacial water pressure [*Kamb et al.,* 1985]; for sub-polar glaciers there is also a cyclic variation in thermal structure [*Clarke and Blake,* 1991]. All of these factors are highly favorable to the sediment entrainment mechanisms depicted in Figure 9. As discussed above, surging is a hydrological instability and, for ice streams, bottom melting is necessary to activate fast flow. A possible shortcoming of surging as an explanation of Heinrich events is that bottom melting erodes ice-entrained sediment and, during fast flow episodes, frictional bottom melting could be very high. It is possible that this problem is less serious than might be imagined. Fast flowing ice streams can become largely decoupled from their beds, restraint being provided by the ice stream margins rather than bed friction. In this way, fast flow and modest bottom melting rates might be reconciled.

The ice shelf breakup mechanism does not invoke fast-flow processes and therefore does not require or provoke large cyclic variations in basal stress, temperature, and water pressure. The absence of fast flow is advantageous for sediment retention and, as suggested by *Hulbe* [1997], ice accretion beneath a floating ice shelf would defend entrained sediment from the initial consequences of berg melting. The problem with the ice shelf breakup mechanism is that it relies entirely on normal rates of sediment entrainment and it is our conviction that normal rates cannot explain the volume of sediment delivered to the North Atlantic during Heinrich events. Finally, Heinrich event H0, though it may not be representative, is known to have been associated with an abrupt advance, not a retreat, of Hudson Strait Ice Stream [*Kaufman et al.*, 1993]. This behavior is consistent with the surging mechanism and inconsistent with ice shelf breakup.

Tidewater instability, as manifested in the recent catastrophic retreat of Columbia Glacier, involves similar stress and hydrological cycles to those associated with the surge instability. For tidewater disintegration of an ice stream, thermal cycling similar to that experienced by a surging ice stream, would also occur. In our opinion, both surging and tidewater instability are equally viable in terms of the criteria presented above.

A POSSIBLE MECHANISM FOR FAST SURFACE-TO-BED COUPLING

If we accept that Heinrich events are initiated by fast motion of the Hudson Strait Ice Stream and that fast flow must result from the triggering of an intrinsic instability, several problems remain. For an instability to be triggered, the system must be near an instability threshold prior to receiving the *coup de grâce*. Why does the instability tend to be triggered during cooling excursions of Dansgaard-Oeschger oscillations? Such behavior suggests that the ice stream is "sensitive", already primed for instability, and argues for the existence of a mechanism for fast coupling between the ice stream surface and its bed. As suggested in a previous section, the only viable fast coupling mechanisms are mechanical. An increase in ice thickness or surface slope will be immediately expressed as an increase in basal shear stress $\tau_B = \rho_I g H_I \sin\theta$ where $g = 9.80\,\mathrm{m\,s^{-2}}$ is the gravitational acceleration and θ is the surface slope. The nonlinear flow law of ice implies that for a simple inclined ice slab the discharge Q_I resulting from ice creep varies strongly with ice thickness. For an $n = 3$ flow law [see *Paterson*, 1994, pp. 95-98] $Q_I \propto H_I^5$, but even vigorous activation of the creep process is unlikely to produce a substantial flow response. For initiation of fast flow, a hydrological response of the bed is far more effective than a purely mechanical response.

One avenue that has not been explored is the possible role of strain heating and creep instability [*Clarke et al.*, 1976; *Yuen and Schubert*, 1979] in mediating a fast coupling between the surface and bed. Before delving into this matter we review some elementary glaciology. The geophysical classification of glaciers, introduced by *Ahlmann* [1935], categorizes glaciers according to their thermal structure. Polar glaciers, the coldest, are everywhere below their melting temperature (Figure 10a); sub-polar glaciers reach the melting temperature at the bed but are otherwise cold (Figure 10b); temperate glaciers are at the melting temperature throughout their entire thickness (Figure 10d). For ice, the melting temperature decreases with increasing pressure so that $T_M = -c_t \rho_I g H_I$ where $c_t = 7.42 \times 10^{-8}\,\mathrm{K\,Pa^{-1}}$ is the pressure melting coefficient. Thus, for example, beneath a 1000 m ice column the melting temperature is $T_M = -0.65°\mathrm{C}$. Years after Ahlmann's system was established, applied mathematicians [*Fowler and Larsen*, 1978; *Hutter*, 1982] pointed to the logical necessity of an intermediate category between sub-polar and temperate glaciers; such glaciers are referred to as polythermal (Figure 10c) and their existence has been observationally confirmed [*Classen*, 1977; *Blatter and Kappenberger*, 1988].

Traditionally those interested in thermal instability of ice sheets have concentrated on triggering a transition from polar to sub-polar thermal regimes [e.g., *Clarke*, 1976; *Clarke et al.*, 1977; *MacAyeal*, 1993a,b]. This fascination is a legacy of the belief that the onset of sliding necessarily accompanies the transition from a cold to melting bed. The transition from sub-polar to polythermal conditions has no effect on bottom temperature, but a closer examination will show that this transition can have an important effect on subglacial hydrological

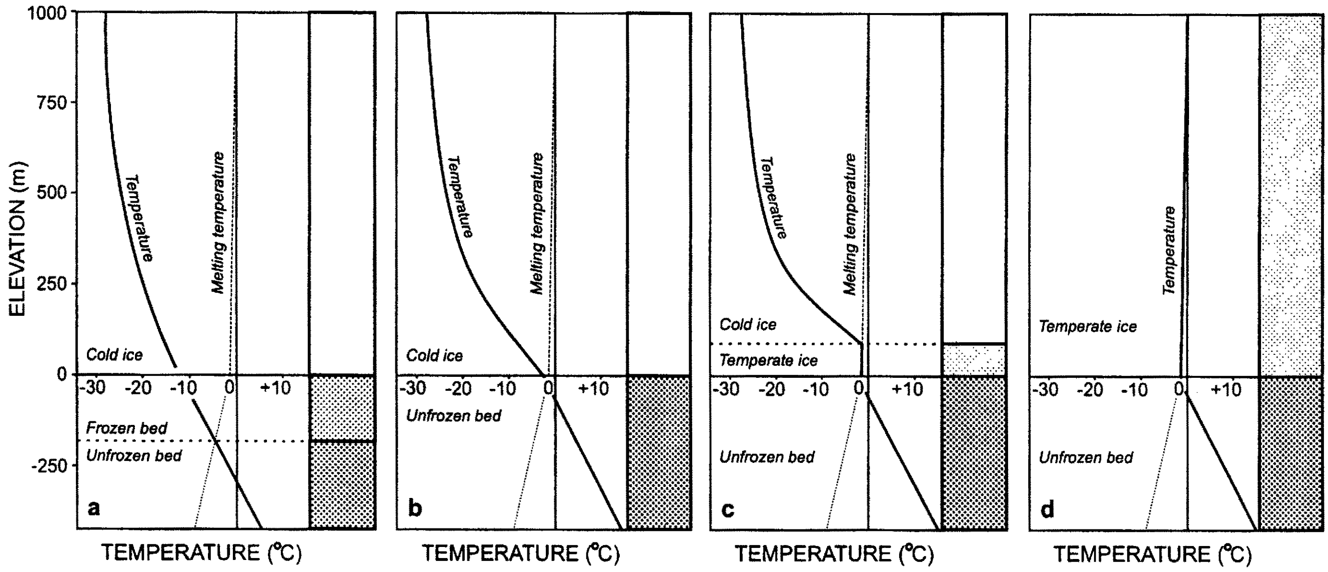

Figure 10. Thermal classification of glaciers and ice sheets. (a) Polar. (b) Sub-polar. (c) Polythermal. (d) Temperate.

conditions and thus could be the agent promoting the transition from slow to fast flow.

For one-dimensional heat transport in an ice column overlying a non-deforming bed, the governing equations for temperature $T = T(z,t)$ are

$$\rho_I c_I \frac{\partial T}{\partial t} = K_I \frac{\partial^2 T}{\partial z^2} - \rho_I c_I v \frac{\partial T}{\partial z} + \Phi \qquad (5a)$$

$$\rho_E c_E \frac{\partial T}{\partial t} = K_E \frac{\partial^2 T}{\partial z^2} \qquad (5b)$$

where Equation (5a) applies in ice and (5b) in the bed, c_I is the specific heat capacity of ice, ρ_E and c_E are the density and specific heat capacity of the bed, v is the bed-normal component of ice velocity, and Φ is the frictional dissipation of the deforming ice. We make standard simplifying assumptions and, taking $z = 0$ to correspond to the ice–bed contact, write $v = -v_0 z/H_I$, $\tau_B = \rho_I g H_I \sin\theta$, and

$$\Phi(z,t) = 2B_0 \exp(-Q/RT)\tau_B^{n+1}[1 - z/H_I(t)]^{n+1} \qquad (6)$$

where B_0 is a constant coefficient, Q is the creep activation energy for ice and $n \sim 3$ is the exponent in Glen's flow law. For appropriate values of B_0 and Q the reader is referred to *Paterson* [1994, p. 97]. The assumed form for τ_B greatly simplifies the mathematical treatment but eliminates interesting and realistic possibilities involving mechanical decoupling of the bed and the accompanying transfer of longitudinal stress.

Intriguing features of (6) are the presence of a positive feedback (the greater the temperature the greater the strain heating), the concentration of frictional dissipation near the ice–bed contact, and the strong dependence of strain heating on ice thickness.

We shall assume that the thickness of the ice slab varies with time in response to changes in the ice-equivalent surface accumulation rate $b(t)$ and take

$$b(t) = b_0 + \frac{1}{2}\Delta b \sin(2\pi t/\Delta t). \qquad (7)$$

If v_0 is assumed to be constant then

$$\frac{dH_I}{dt} = -v_0 + b(t). \qquad (8)$$

With the foregoing assumption, the ice column can thicken or thin depending on the relative magnitudes of v_0 and b; as thickness changes so does the magnitude of the strain heating term. The dimensionless Brinkman number, here defined as

$$\mathrm{Br}(t) = \frac{H_I(t)\Phi(0,t)}{K_I T(0,t)}, \qquad (9)$$

with T expressed as absolute temperature, is a useful indicator of the significance of strain heating. In our work, Br = 1 roughly delineates the threshold between low and high Brinkman numbers.

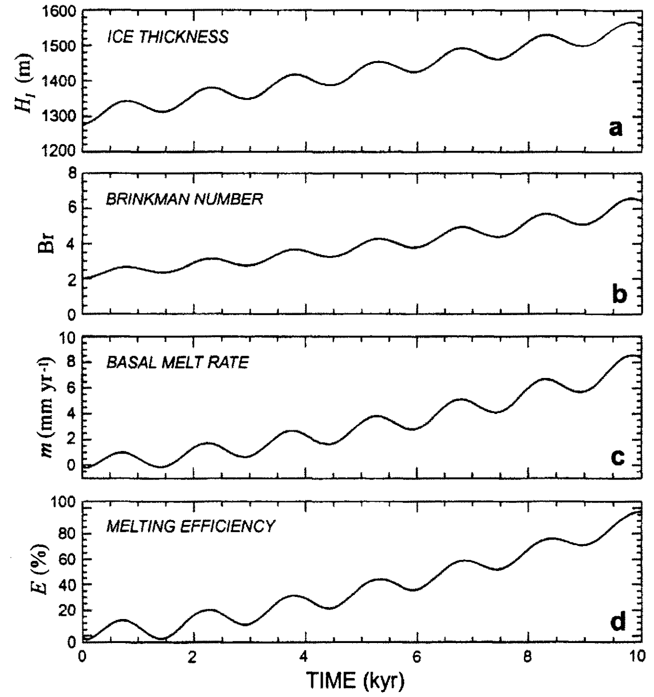

Figure 11. Time evolution of one-dimensional thermal model. (a) Ice thickness. (b) Brinkman number. (c) Basal melting rate. (d) Melting efficiency parameter.

Equations (5a) and (5b) are subject to boundary conditions and initial conditions. For simplicity we assume that at $t = 0$ the system is in a steady-state. As boundary conditions we take $\partial T/\partial z = -q_G/K_E$ at the lower boundary where q_G is the geothermal flux and $T(H_I, t) = T_S(t)$ at the upper boundary, where $T_S(t)$ is a specified surface temperature variation. At the ice–bed contact

$$-K_E \frac{\partial}{\partial z} T(0^-, t) + K_I \frac{\partial}{\partial z} T(0^+, t) = 0 \qquad (10)$$

if the bed temperature is below the melting temperature, and $T(0, t) = -c_t \rho_I g H_I(t)$ if the bed is at the melting temperature. If the bed is at the melting temperature and sliding friction is neglected then, with $n_I = 1$, Equation (2) gives the basal melting rate as

$$\dot{m} = \frac{1}{\rho_I L} \left\{ -K_E \frac{\partial}{\partial z} T(0^-, t) + K_I \frac{\partial}{\partial z} T(0^+, t) \right\}. \qquad (11)$$

Figure 11 shows a computer simulation of the effects of strain heating on melt generation in an ice column subjected to a time-varying surface accumulation rate. Because we have taken $b_0 > v_0$ the long-term trend is for ice thickness to increase with time. A sinusoidal fluctuation in b, of period 1 kyr, accounts for the sinusoidal fluctuation in ice thickness (Figure 11a). Figure 11b shows, not surprisingly, that sinusoidal fluctuations in Brinkman number are synchronized with thickness variations. Furthermore, time variation in strain heating gives rise to a synchronous variation in the basal melt rate (Figure 11c). This effect can be expressed in terms of time variations in a melting efficiency parameter defined as $E = 1 - q^+/q^-$ where $q^+ = -K_I \partial T(0^+, t)/\partial z$ and $q^- = -K_E \partial T(0^-, t)/\partial z$. The inequality $0 < E < 1$ defines the existence region for sub-polar glaciers. At lower levels of strain heating than those consistent with $0 < E < 1$ the thermal regime is polar; at higher levels of strain heating than those consistent with this inequality, the thermal regime is polythermal or temperate. Polar, polythermal, and temperate glacier types can be viewed as insensitive because subglacial melt production is unaffected by ice thickness fluctuations.

Figure 12 illustrates how sensitivity is achieved. The results are extracted from the simulation that yielded Figure 11 and focuses attention on conditions near the ice–bed contact. The temperature vs. depth curves (Figure 12a) are for times $t = 0$ kyr (solid line), $t = 6.5$ kyr (dot-dashed line), and $t = 10$ kyr (dotted line). The melting efficiencies at these times are roughly 0%, 50%, and 100%. Figure 12b shows the vertical distribution of heat flux at the same time snapshots. The solid line ($E \approx 0\%$) shows a continuous variation in heat flux as the ice–bed contact is traversed, implying that no portion of the inflowing heat flux is available for

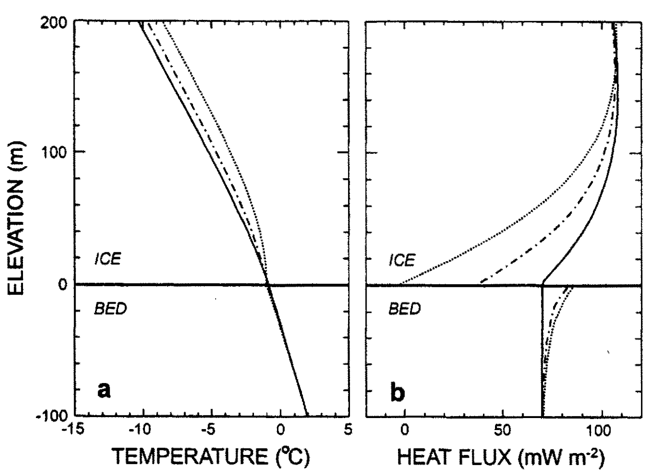

Figure 12. Results of one-dimensional thermal model showing switching from sub-polar to polythermal regime. (a) Temperature distribution. (b) Heat flux distribution.

meltwater production. The dot-dashed line ($E \approx 50\%$) shows a sharp discontinuity in heat flux across the ice–bed boundary, and the dotted line ($E \approx 100\%$) shows an even more pronounced discontinuity. Temporal and spatial variation in the subglacial heat flux are a consequence of the change in melting temperature associated with a thickening ice column.

Critical State Conjecture and Its Attractions

We have demonstrated that a sub-polar ice mass having a high Brinkman number is in a sensitive state. Changes in ice thickness or surface slope are immediately communicated to the bed as changes in basal stress τ_B and, through (6), these are transformed to strain heating at the bed and increased basal meltwater production. If the Hudson Strait Ice Stream was sensitive in this way, atmospheric forcing (e.g., increased accumulation rate leading to increased ice thickness) and a flow response could become phase-locked and an extreme forcing could, plausibly, launch one of several possible flow instabilities. Sensitivity alone seems incapable of explaining the vigorous ice discharge associated with Heinrich events; an instability must be triggered.

Rather than dismiss sensitivity as an unique feature of Hudson Strait Ice Stream, we propose that under certain circumstances it could be a commonplace one. As cold glaciers and ice sheets thicken, they change from a predominantly polar thermal regime (Figure 10a) to a predominantly sub-polar thermal regime (Figure 10b). By itself this transition is not likely to be accompanied by a dramatic change in flow rate, thus thickening might continue until strain heating became strong enough to render the ice mass sensitive and thus responsive to changes in surface loading. This line of thought is reminiscent of self-organized criticality [*Bak et al.*, 1987, 1988] and it is our conjecture that, during epochs when global ice volume is increasing, a substantial fraction of the existing glaciers and ice sheets evolve to a sensitive state. If this speculation is correct then the seemingly paradoxical evidence for a quasi-synchronous climate-orchestrated response of unlinked glacial systems [e.g., *Elliot et al.*, 1998; *Grousset et al.*, 1998; *van Kreveld et al.*, 1998] might be explained.

We offer no proof of these assertions but believe they are amenable to testing using appropriately designed computer models. Indeed, self-organization, though not self-organized criticality, has been demonstrated by the three-dimensional thermomechanical ice sheet model of *Payne and Dongelmans* [1997].

MODELING OF SURGING AND TIDEWATER INSTABILITY MECHANISMS

Computer modeling has provided a valuable tool for examining the viability of glaciological models of Hudson Strait ice dynamics. Reduced models [*MacAyeal*, 1993a,b; *Verbitsky and Saltzman*, 1995] are useful for isolating process interactions and identifying promising research directions. Flow-line models [*Greve and MacAyeal*, 1996] and non-thermodynamic two-dimensional flow models [*Pfeffer et al.*, 1997] add realism without making unreasonable demands on computing power. The first attempt to embed surges of Hudson Strait Ice Stream within a full thermomechanical model of Laurentide Ice Sheet dynamics is described by *Marshall and Clarke* [1997a,b]. Sensitivity, in the sense we have discussed, is not a feature of the Marshall and Clarke (MC) model nor of other conventional ice dynamics models. Indeed sensitivity presents a modeling challenge because the phenomenon is associated with a thermal boundary layer and these are poorly resolved by existing coarse-gridded thermomechanical models.

Details of the MC ice stream surge model are fully described in *Marshall and Clarke* [1997b] and here we simply review the main results. Figure 13 shows the ice surface topography and barycentric ice surface velocity predicted by the MC reference model 1 kyr after the surge onset. The fast flow channel through Hudson Strait is clearly apparent from the velocity vectors (Figure 13b) as is the deflection of flow from surrounding sheet ice toward the ice stream. For this model the calculated surge duration was 750 yr and the duration of the quiescent period was found to be 4500 yr, values that are broadly consistent with those extracted from the paleoceanographic record. The maximum outlet velocity was found to be 3320 m yr^{-1}, considerably less the 18000 m yr^{-1} predicted by *MacAyeal's* [1993b] binge/purge model. Similarly the predicted freshwater flux (icebergs plus meltwater) for the MC reference model is 102 $\mathrm{km}^3\,\mathrm{yr}^{-1}$ (0.0032 Sv) in contrast to MacAyeal's value of 2479 $\mathrm{km}^3\,\mathrm{yr}^{-1}$ (0.079 Sv). Even the MC maximum model [*Marshall and Clarke*, 1997b], aimed at placing physically reasonable upper limits on flow velocity (6680 m yr^{-1}) and freshwater discharge (278 $\mathrm{km}^3\,\mathrm{yr}^{-1}$ or 0.0088 Sv) falls far short of the binge/purge predictions. Other points of comparison are provided by freshwater discharge estimates based on ocean sedimentation measurements and with the results of ocean dynamics modeling experiments. The net freshwater flux of the MC maximum model compares very

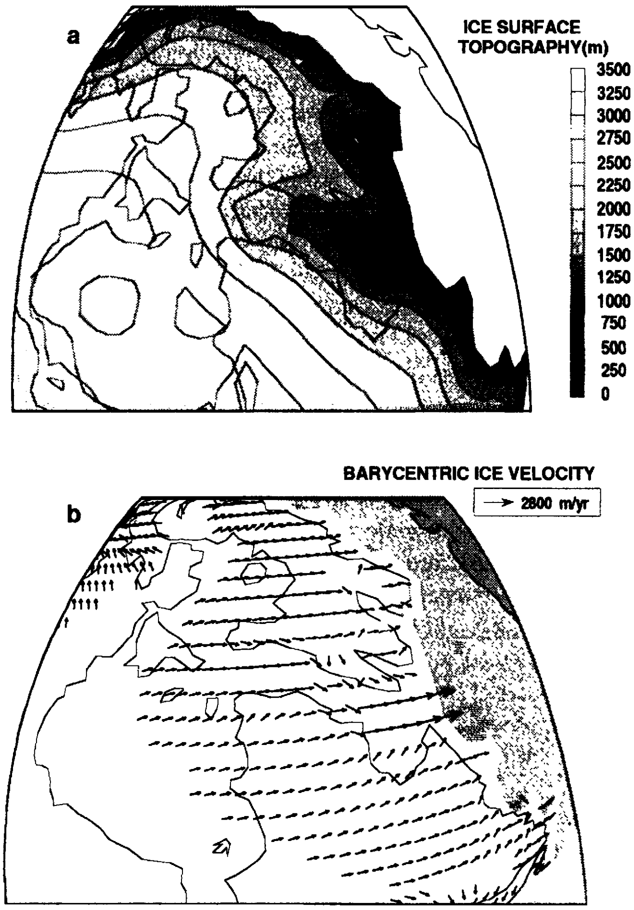

Figure 13. Model of Hudson Strait Ice Stream surge. (a) Ice surface topography 1 kyr after surge onset. (b) Barycentric (a weighted average) ice surface velocity 1 kyr after surge onset.

favorably to that estimated by *Dowdeswell et al.* [1995] based on measurements of the thickness of ice-rafted sediment for events H1 and H2. Several ocean dynamics modeling studies have explored the effect on thermohaline circulation (THC) of increased freshwater input to the North Atlantic. *Rahmstorf* [1995] examined bifurcations in the equilibrium response rather than sensitivity to event-like disturbances; he found that an increase of 0.075 Sv was sufficient to switch the THC from its present value of ~17 Sv to essentially full shutdown. *Manabe and Stouffer* [1995] assumed a 1 Sv increase in freshwater input, sustained for 10 yr, and triggered an abrupt weakening in THC followed by a complicated response. The study of *Weaver* [this volume] is most directly relevant to Heinrich events and is based on the MC estimates of freshwater flux. For the MC reference model the THC decreases from an LGM rate of 11 Sv to ~5 Sv; for the maximum model the rate drops to ~3.5 Sv.

The MC reference model predicts cyclic oscillations in geometry, temperature, and flow rate (Figure 14) for a constant climate. Figure 14a shows the simulated ice velocity at Hudson Strait outlet. At the surge onset, velocity rapidly increases from near zero to 3320 m yr^{-1} then slowly decreases to around 1800 m yr^{-1} before the surge abruptly shuts down. Basal temperature also

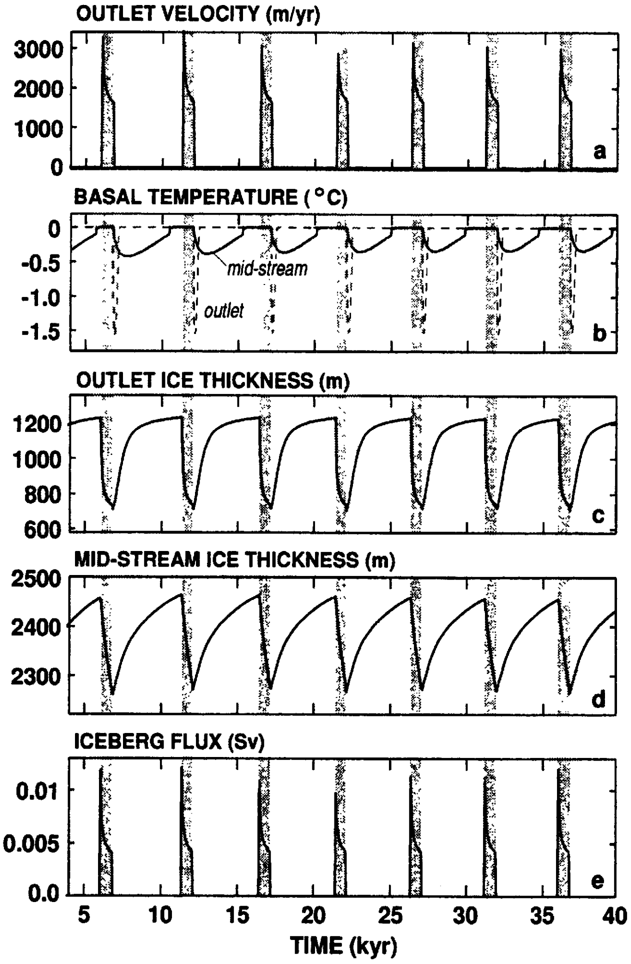

Figure 14. Time series results of Hudson Strait Ice Stream surge model. (a) Ice surface velocity at the ice stream outlet. (b) Basal temperature at the ice stream outlet and at a site halfway between the outlet and the head of the ice stream. (c) Ice thickness at the ice stream outlet. (d) Ice thickness at a site halfway between the outlet and the head of the ice stream. (e) Iceberg flux from ice stream.

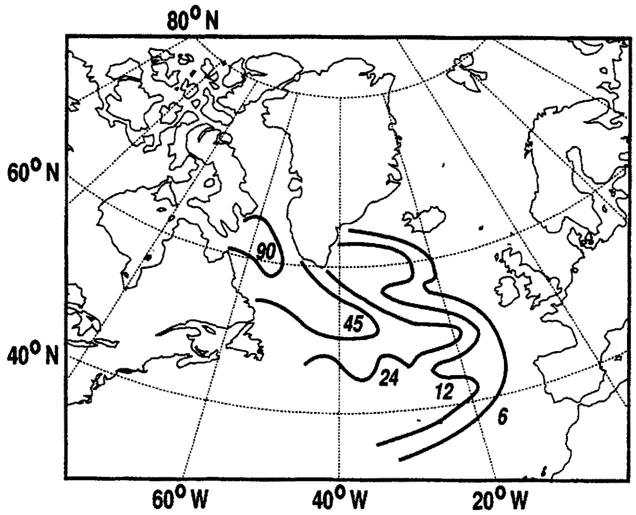

Figure 15. Iceberg melt rates (in cm yr^{-1} water equivalent) based on computer model of Hudson Strait Ice Stream surge and the sedimentation estimates of *Dowdeswell et al.* [1995].

varies cyclically (Figure 14b) along the length of the ice stream. During the active phase of a surge, the bed temperature is at the melting point. At the ice stream outlet, where thickness variations are the most extreme, the temperature swing is 1.5°C. The ice thickness variation at the outlet (Figure 14) is roughly 450 m whereas halfway toward the head of the ice stream the thickness variation is only 200 m (Figure 14d). The predicted iceberg discharge (expressed in Sverdrups) is shown in Figure 14e.

Our success in modeling cyclic surging of Hudson Strait Ice Stream lends credibility to the claim that surges are a viable causative mechanism for Heinrich events, as first proposed by *MacAyeal* [1993b]. A second application of the model is to predict the discharge and total volume of icebergs and freshwater to the North Atlantic Ocean (Figure 14e). As yet the MC continental ice dynamics model has not been coupled to an iceberg transport model so the areal distribution of freshwater flux, an important forcing for ocean circulation models, is not predicted. As an interim measure we use Heinrich sedimentation estimates [*Dowdeswell et al.*, 1995] as a proxy for iceberg melt, and areally distribute the iceberg water flux predicted by the MC model in proportion to the IRD sedimentation estimates. Figure 15 shows the results of this calculation. The reader is referred to *Weaver* [this volume] for the results of computer simulations of the ocean circulation response to this freshwater forcing.

The MC model has also been used to examine whether tidewater instability is a viable glaciological mechanism for explaining Heinrich events. Models of this kind are extremely sensitive to the form of the calving law as well as to the magnitude of the rate constant k_c in Equation (1); by choosing a large value for the rate constant, vigorous calving can be promoted. Figure 16 shows how vigorous calving affects the growth of the North American ice sheet. Here the MC model is forced by a climate model controlled by the GRIP $\delta^{18}O$ record [*Dansgaard et al.*, 1993] and GCM temperature and P–E fields computed for present day and last glacial maximum (LGM) climate using the CCCv2.0 model of the Canadian Climate Centre for Modelling and Analysis. Details are given in *Marshall et al.* [submitted]. The ice dynamics simulation is started at 120 kyr BP from a fully-deglaciated state and integrated forward to the present day. At 50 kyr (Figures 16a and 16b) much of Hudson Bay remains ice-free and open to the Labrador Sea. By 40 kyr (Figure 16c) this embayment has been greatly reduced and by 20 kyr (the LGM) it has disappeared entirely (Figure 16d). One immediate conclusion of this modeling exercise is that it would be difficult to justify a more vigorous calving law than that employed for this simulation because more vigorous calving would further delay or prevent ice coverage of Hudson Bay.

Close examination of these simulation results reveals that minor fluctuations of the Hudson Strait calving margin occur as the large-scale trends of infilling and formation of an ice dome proceed. Figure 17 shows the changes in surface topography, ice thickness, surface velocity, and the sum of basal and internal melt rates that accompany one such fluctuation. The values presented in this figure are obtained by averaging modeling results over the latitude range 60–64°N (six cell widths). The calving front retreat of 2° longitude (~110 km) occurs over the time interval 20 kyr to 16 kyr. In fact the active retreat occurs over a much smaller time interval, from 18.00 kyr to 17.95 kyr. The rapid 200 km retreat of a tidewater glacier would, by modern measures, seem impressive. Relative to the ice volume requirements of Heinrich events, the simulated tidewater retreat is completely inadequate.

Our modeling results raise serious questions about the viability of tidewater disintegration as an explanation of large episodic iceberg fluxes from Hudson Strait. A more vigorous calving law might promote a more impressive retreat of the calving margin but would also delay or entirely prevent the formation of an ice dome covering Hudson Bay. One could escape this difficulty by switching between a weak and strong calving law

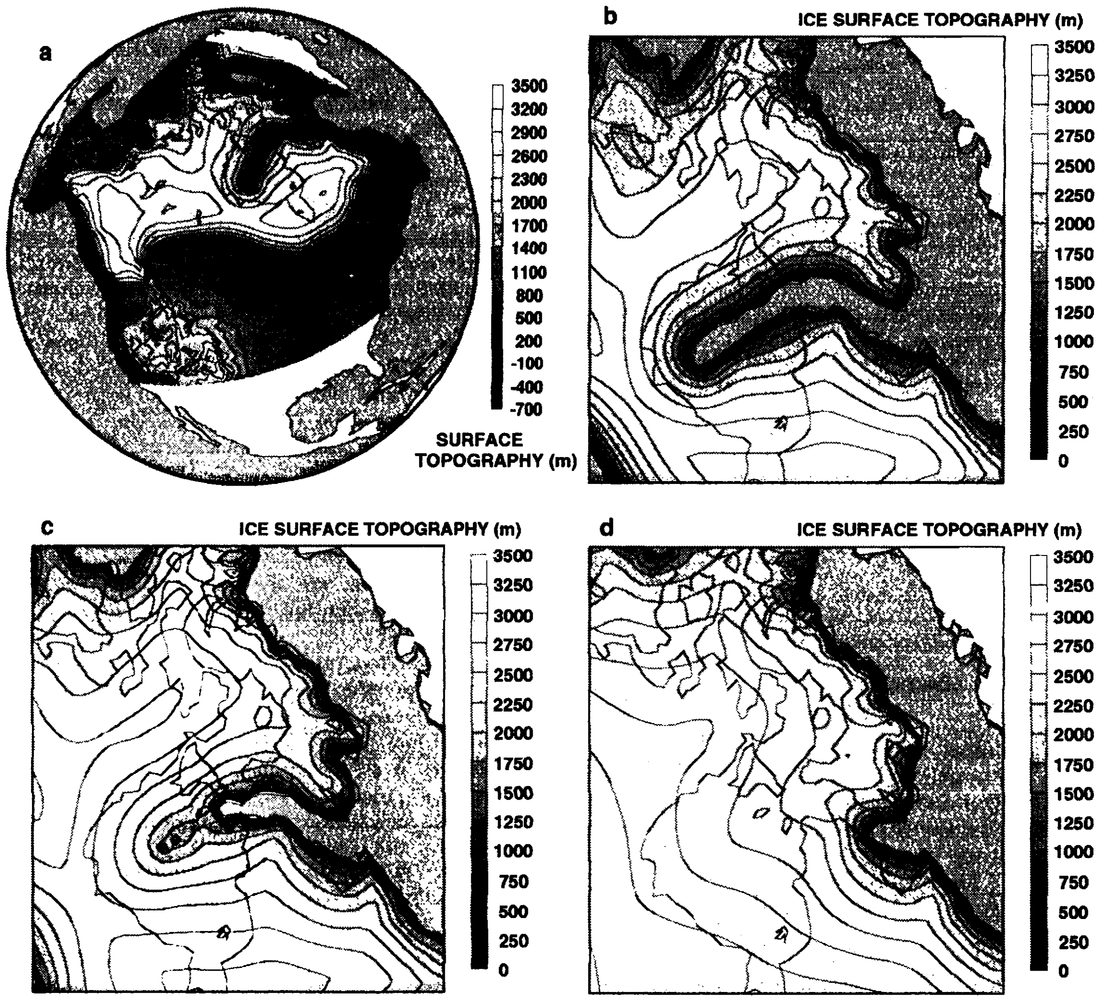

Figure 16. Evolution of North American Ice Sheet if vigorous calving is assumed. (a) Map of North American Ice Sheet at 50 kyr BP. (b) Detail of ice distribution in Hudson Strait region at 50 kyr BP. (c) Detail of ice distribution in Hudson Strait region at 40 kyr BP. (d) Detail of ice distribution in Hudson Strait region at 20 kyr BP.

but this "hand-of-God" expedient has no clear physical justification. Given the state of knowledge of calving physics and the subgrid nature of the processes governing calving and grounding line retreat, it is premature to dismiss the tidewater instability mechanism.

CONCLUSIONS

The paleoceanographic record at Orphan Knoll supports the assertion that there is no premonitory climate signal associated with Heinrich events. The first expression of Heinrich event onset is increased submarine sediment transport along the Northwest Atlantic Mid-Oceanic Channel that links the ice source at Hudson Strait with the Orphan Knoll core site. A delayed Heinrich event signal is the increased sedimentation of ice-rafted debris and dilution of near-surface waters by iceberg melt. "Normal" ice sheet and ice stream flow rates are believed to be insufficient for explaining the large volumes of ice and sediment exported by Heinrich events. It is therefore likely that the onset of a Heinrich event occurs when a glacier flow instability is triggered. Based on our assessment of the merits and shortcomings of candidate instability mechanisms as well as attempts to model the surging and tidewater instability mechanisms, the preferred explanation of increased ice flux through Hudson Strait is that Hudson Strait Ice Stream surges episodically. Although small-scale tidewater instability events can be simulated, large-scale instability is difficult or impossible to excite unless we manipulate

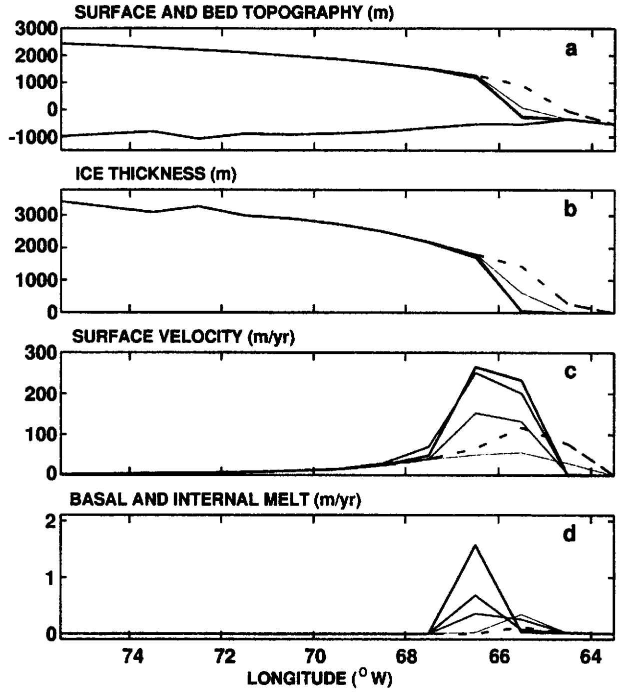

Figure 17. Time slices showing the occurrence of tidewater instability. The simulation run is the same as used to generate Figure 16 and assumes an extremely vigorous calving law. Plotted values are obtained by averaging simulation results over the latitude interval 60–64°N. (a) Surface and bed topography. (b) Ice thickness. (c) Surface velocity. (d) Basal and internal melt rates.

the ice calving law. Incomplete understanding of the calving process, rather than non-viability of the tidewater instability mechanism, may lie at the heart of this difficulty. Finally, we speculate that during the build-up to a Heinrich event, phase-locking between an atmospheric forcing applied to the ice surface and subglacial meltwater production, a necessary process for activating fast flow, can be achieved if the ice mass is in sensitive condition, i.e., if the ice–bed contact is at the melting temperature and strain heating is appreciable.

Acknowledgments. This paper is a contribution to Phase 2 of the Climate System History and Dynamics Program (CSHD) that is jointly sponsored by the Natural Sciences and Engineering Research Council of Canada (NSERC) and the Atmospheric Environment Service of Canada. We greatly appreciate the helpful criticism of Tad Pfeffer and an anonymous reviewer whose comments have substantially improved this submission.

REFERENCES

Ahlmann, H. W., Contribution to the physics of glaciers, *Geogr. J., 86*, 97-113, 1935.

Alley, R. B., Water-pressure coupling of sliding and bed deformation: II. Velocity-depth profiles, *J. Glaciol., 35*(119), 119-129, 1989.

Alley, R. B., Sedimentary processes may cause fluctations of tidewater glaciers, *Ann. Glaciol., 15*, 119-124, 1991.

Alley, R. B., and D. R. MacAyeal, Ice-rafted debris associated with binge/purge oscillations of the Laurentide Ice Sheet, *Paleoceanography, 9*(4), 503-511, 1994.

Andrews, J. T., Abrupt changes (Heinrich events) in late Quaternary North Atlantic marine environments: a history and review of data and concepts, *J. Quat. Sci., 13*(1), 3-16, 1998.

Andrews, J. T., K. Tedesco, and A. E. Jennings, Heinrich events: chronology and processes, east-central Laurentide Ice Sheet and NW Labrador Sea, in *Ice in the Climate System,* edited by W. R. Peltier, pp. 167-186, Springer-Verlag, Berlin, 1993.

Andrews, J. T., K. Tedesco, W. M. Briggs, and L. W. Evans, Sediments, sedimentation rates, and environments, southeast Baffin Shelf and northwest Labrador Sea, 8–26 ka, *Can. J. Earth Sci., 31,* 90-103, 1994.

Bak, P., C. Tang, and K. Wiesenfeld, Self-organized criticality: An explanation of $1/f$ noise, *Phys. Rev. Lett., 59,* 381-384, 1987.

Bak, P., C. Tang, and K. Wiesenfeld, Self-organized criticality. *Phys. Rev. A, 38,* 364-374, 1988.

Blatter, H., and Kappenberger, G., Mass balance and thermal regime of Laika Ice Cap, Coburg Island, N.W.T., Canada, *J. Glaciol., 34,* 102-110, 1988.

Bond, G. C., and R. Lotti, Iceberg discharges into the North Atlantic on millenial time scales during the last glaciation, *Science, 267,* 1005-1010, 1995.

Bond, G., H. Heinrich, W. Broecker, L. Labeyrie, J. McManus, J. Andrews, S. Huon, R. Jantschik, S. Clasen, C. Simet, K. Tedesco, M. Klas, G. Bonani, and S. Ivy, Evidence for massive discharges of icebergs into the North Atlantic ocean during the last glacial period, *Nature, 360,* 245- 249, 1992.

Bond, G., W. Broecker, S. Johnsen, J. McManus, L. Labeyrie, J. Jouzel, and G. Bonani, Correlations between climate records from North Atlantic sediments and Greenland ice, *Nature, 365,* 143-147, 1993.

Bond, G., W. Showers, M. Cheseby, R. Lotti, P. Almansi, P. deMenocal, P. Priore, H. Cullen, I. Hajdas, and G. Bonani, A pervasive millenial-scale cycle in North Atlantic Holocene and glacial climates, *Science, 278,* 1257-1266, 1997.

Broecker, W. S., Massive iceberg discharges as triggers for global climate change, *Nature, 372,* 421-424, 1994.

Broecker, W., G. Bond, M. Klas, E. Clark, and J. McManus, Origin of the northern Atlantic's Heinrich events, *Clim. Dyn., 6,* 265-273, 1992.

Brown, C. S., W. G. Sikonia, A. Post, L. A. Rasmussen, and M. F. Meier, Two calving laws from grounded iceberg-calving glaciers, *Ann. Glaciol., 4,* 295, 1983.

Clarke, G. K. C., Thermal regulation of glacier surging, *J. Glaciol., 16*(74), 231-250, 1976.

Clarke, G. K. C., and E. W. Blake, Geometric and thermal evolution of a surge-type glacier in its quiescent state: Trapridge Glacier 1969–89, *J. Glaciol., 37*(125), 158-169, 1991.

Clarke, G. K. C., U. Nitsan, and W. S. B. Paterson, Strain heating and creep instability in glaciers and ice sheets, *Rev. Geophys.*, *15*(2), 235-247, 1977.

Classen, D. F., Temperature profiles for the Barnes Ice Cap surge zone, *J. Glaciol.*, *18*, 391-405, 1977.

Clayton, L., J. T. Teller, and J. W. Attig, Surging of the southwestern part of the Laurentide ice sheet, *Boreas*, *14*, 235-242. 1985.

Dansgaard, W., et al., Evidence for general instability of past climate from a 250-kyr ice-core record, *Nature*, *364*, 218-220, 1993.

Doake, C. S. M., H. F. J. Corr, H. Rott, P. Skvarca, and N. W. Young, Breakup and conditions for stability of the northern Larsen Ice Shelf, Antarctica, *Nature*, *391*, 778-780, 1998.

Dowdeswell, J. A., M. A. Maslin, J. T. Andrews, and I. N. McCave, Iceberg production, debris rafting, and the extent and thickness of Heinrich layers (H-1, H-2) in North Atlantic sediments, *Geology*, *23*(4), 301-304, 1995.

Elliot, M., L. Labeyrie, G. Bond, E. Cortijo, J.-L. Turon, N. Tisherat, and J.-C. Duplessy, Millenial-scale iceberg discharges in the Irminger Basin during the last glacial period: Relationship with the Heinrich events and environmental settings, *Paleoceanography*, *13*, 433-446, 1998.

Fowler, A. C., and D. A. Larson, On the flow of polythermal glaciers I. Model and preliminary analysis. *Proc. R. Soc. London A*, *363*, 217-242, 1978.

Greve, R., and D. R. MacAyeal, Dynamic/thermodynamic simulations of Laurentide ice-sheet instability, *Ann. Glaciol.*, *23*, 328-335, 1996.

Grousset, F. E., H. Snoeckx, and M. Revel, Did the European Ice Sheet surges trigger the North Atlantic Heinrich events? Poster presentation at AGU Chapman Conference on "Mechanisms of Millenial-Scale Global Climate Change", Snowbird, Utah, June 14-18, 1998.

Gwiazda, R. H., S. R. Hemming, and W. S. Broecker, Tracking the sources of icebergs with lead isotopes: The provenance of ice-rafted debris in Heinrich layer 2, *Paleoceanography*, *11*, 77-93, 1993a.

Gwiazda, R. H., S. R. Hemming, and W. S. Broecker, The provenance of icebergs during in Heinrich event 3 and the contrast to their sources during other Heinrich episodes, *Paleoceanography*, *11*, 371-378, 1993b.

Heinrich, H., Origin and consequences of cyclic ice rafting in the Northeast Atlantic Ocean during the past 130,000 years, *Quat. Res.*, *29*, 142-152, 1988.

Hesse, R., and A. Rakofsky, Deep-sea channel/submarine-Yazoo system of the Labrador Sea: a new deep-water facies model, *Amer. Assoc. Petrol. Geol. Bull.*, *76*, 680-707, 1992.

Hillaire-Marcel, C., A. de Vernal, G. Bilodeau, and G. Wu, Isotope stratigraphy, sedimentation rates, deep circulation, and carbonate events in the Labrador Sea during the last ~200 ka, *Can. J. Earth Sci.*, *31*, 63-89, 1994a.

Hillaire-Marcel, C., A. de Vernal, M. Lucotte, A. Mucci, G. Bilodeau, A. Rochon, S. Vallières, and G.-P. Wu, Productivité et flux de carbone dans la mer du Labrador au cours des derniers 40 000 ans, *Can J. Earth Sci.*, *31*, 139-158, 1994b.

Hulbe, C. L., An ice shelf mechanism for Heinrich layer production, *Paleoceanography*, *12*(5), 711-717, 1997.

Hunt, A. G., and P. E. Malin, Possible triggering of Heinrich events by ice-load-induced earthquakes, *Nature*, *393*, 155-158, 1998.

Hutter, K., A mathematical model of polythermal glaciers and ice sheets. *Geophys. Astrophys. Fluid Dynamics*, *21*, 201-224, 1982.

Iken, A., and R. A. Bindschadler, Combined measurements of subglacial water pressure and surface velocity of Findelengletscher, Switzerland: conclusions about drainage system and sliding mechanism, *J. Glaciol.*, *32*, 101-119, 1986.

Iverson, N. R., Regelation of ice through debris at glacier beds: Implications for sediment transport, *Geology*, *21*, 559-562, 1993.

Iverson, N. R., and D. J. Semmens, Intrusion of ice into porous media by regelation: A mechanism of sediment entrainment by glaciers, *J. Geophys. Res.*, *100*(B7), 10,219-10,230, 1995.

Iverson, N. R., B. Hanson, R. LeB. Hooke, and P. Jansson, Flow mechanism of glaciers on soft beds, *Science*, *267*, 80-81, 1995.

Kamb, B., Rheological nonlinearity and flow instability in the deforming bed mechanism of ice stream motion, *J. Geophys. Res.*, *96*(B10), 16,585–16,595, 1991.

Kamb, B., C. F. Raymond, W. D. Harrison, H. Engelhardt, K. A. Echelmeyer, N. Humphrey, M. M. Brugman, and T. Pfeffer, Glacier surge mechanism: 1982-1983 surge of Variegated Glacier, Alaska, *Science*, *227*(4686), 469-479, 1985.

Kamb, B., H. Engelhardt, M. Fahnestock, N. Humphrey, M. Meier, and D. Stone, Mechanical and hydrologic basis for the rapid motion of a large tidewater glacier 2. Interpretation, *J. Geophys. Res.*, *99*(B8), 15,231-15,244, 1994.

Kaufman, D. S., G. H. Miller, J. A. Stravers, and J. T. Andrews, Abrupt early Holocene (9.9–9.6 ka) ice-stream advance at the mouth of Hudson Strait, Arctic Canada, *Nature*, *21*, 1063-1066, 1993.

Lucotte, M., and C. Hillaire-Marcel, Identification et distribution des grandes masses d'eau dans les mers du Labrador et d'Irminger, *Can. J. Earth Sci.*, *31*, 5-13, 1994.

MacAyeal, D. R., A low-order model of the Heinrich event cycle, *Paleoceanography*, *8*(6), 767-773, 1993a.

MacAyeal, D. R., Binge/purge oscillations of the Laurentide ice sheet as a cause of the North Atlantic's Heinrich events, *Paleoceanography*, *8*(6), 775-784, 1993b.

Manabe, S., and R. J. Stouffer, Simulation of abrupt climate change induced by freshwater input to the North Atlantic Ocean, *Nature*, *378*, 165-167, 1995.

Marshall, S. J., and G. K. C. Clarke, A continuum mixture model of ice stream thermomechanics in the Laurentide Ice Sheet 1. Theory, *J. Geophys. Res.*, *102*(B9), 20,599-20,613, 1997a.

Marshall, S. J., and G. K. C. Clarke, A continuum mixture model of ice stream thermomechanics in the Laurentide Ice Sheet 2. Application to the Hudson Strait Ice Stream, *J. Geophys. Res.*, *102*(B9), 20,615-20,637, 1997b.

Marshall, S. J., L. Tarasov, G. K. C. Clarke, and W. R. Peltier, Glaciology of Ice Age cycles: Physical processes and modelling challenges, *Can. J. Earth Sci.*, submitted.

Meier, M. F., and A. Post, Fast tidewater glaciers, *J. Geophys. Res.*, *92*(B9), 9051-9058, 1987.

Meier, M., S. Lundstrom, D. Stone, B. Kamb, H. Engelhardt, N. Humphrey, W. W. Dunlap, M. Fahnestock, R.

M. Krimmel, and R. Walters, Mechanical and hydological basis for the rapid motion of a large tidewater glacier 1. Observations, *J. Geophys. Res., 99*(B9), 15,219-15,229, 1994.

Paterson, W. S. B., *The Physics of Glaciers*, Pergamon, Tarrytown, N. Y., 1994.

Paterson, W. S. B., Some aspects of the physics of glaciers, in *Ice Physics in the Natural Environment*, edited by J. S. Wettlaufer, J. G. Dash, and N. Untersteiner, pp. 69-88, NATO Advanced Study Institute, *56, Ser. I*, Springer-Verlag, Berlin, 1998.

Payne, A. J., and P. W. Dongelmans, Self-organization in the thermomechanical flow of ice sheets, *J. Geophys. Res., 102*(B6), 12,219-12,233, 1997.

Pfeffer, W. T., M. Dyurgerov, M. Kaplan, J. Dwyer, C. Sassolas, A. Jennings, B. Raup, and W. Manley, Numerical modeling of late Glacial Laurentide advance of ice across Hudson Strait: Insights into terrestrial and marine geology, mass balance, and calving flux, *Paleoceanography, 12*(1), 97-110, 1997.

Phillip, J. R., Thermal field during regelation, *Cold Regions Sci. Technol., 3*, 193-203, 1980.

Post, A. S., Alaskan glaciers: recent observations in respect to the earthquake-advance theory, *Science, 148*, 366-368, 1965.

Rahmstorf, S., Bifurcations of the Atlantic thermohaline circulation in response to changes in the hydrological cycle, *Nature, 378*, 145-149, 1995.

Raymond, C. F., How do glaciers surge? A review, *J. Geophys. Res., 92*(B9), 9121-9134, 1987.

Raymond, C., T. Johannesson, T. Pfeffer, and M. Sharp, Propagation of a glacier surge into stagnant ice, *J. Geophys. Res., 92*(B9), 9037-9049, 1987.

Reeh, N., On the calving of ice from floating glaciers and ice shelves, *J. Glaciol., 7*, 215-232, 1968.

Reeh, N., C. E. Bøggild, and H. Oerter, Surge of Storstrømmen, a large outlet glacier from the Inland Ice of North-East Greenland, *Rapp. Grønlands geol. Unders., 162*, 201-209, 1994.

Roberts, A. P., B. Lehman, R. J. Weeks, K. L. Verosub, and C. Laj, Relative paleointensity of the geomagnetic-field over the last 200,000 years from ODP sites 883 and 884, North Pacific Ocean. *Earth Planet. Sci. Lett., 152*, 11-23, 1997.

Ruddiman, W. F., Late Quaternary deposition of ice-rafted sand in the subpolar North Atlantic (lat 40° to 65°N), *Geol. Soc. Am. Bull., 88*, 1813-1827, 1977.

Russell-Head, D. S., The melting of free-drifting icebergs, *Ann. Glaciol., 1*, 119-127, 1980.

Saussure, H.-B. de, *Voyages dan les Alpes, précédés d'un essai sur l'histoire naturelle des environs de Geneve* (4 vols.), S. Fauche, Neuchâtel, Switzerland, 1779-96.

Schytt, V., Some comments on glacier surges in eastern Svalbard, *Can. J. Earth Sci., 6*, 867-871, 1969.

Sharp, M. J., 'Crevasse-fill' ridges: a landform type characteristic of surging glaciers? *Geografiska Annaler, 67A*, 213-220, 1985.

Stoner, J. S., J. E. T. Channell, C. Hillaire-Marcel, The magnetic signature of rapidly deposited detrital layers from the deep Labrador Sea: Relationship to North Atlantic Heinrich layers, *Paleoceanography, 11*(3), 309-325, 1996.

Stoner, J. S., J. E. T. Channell, and C. Hillaire-Marcel, A 200 ka geomagnetic chronostratigraphy for the Labrador Sea: Indirect correlation of the sediment record to SPECMAP, *Earth Planet. Sci. Let.*, 165-181, 1998.

Tarr, R. S., and L. Martin, *Alaska Glacier Studies*, National Geographic Society, Washington, D.C., 1914.

van Kreveld, S., U. Pflaumann, M. Sarnthein, P. Grootes, and M. J. Nadeau, Correlation between temperature records from Reykjanes Ridge sediment and GISP2 ice-core, Poster presentation at AGU Chapman Conference on "Mechanisms of Millenial-Scale Global Climate Change", Snowbird, Utah, June 14-18, 1998.

Veiga-Pires, C., and C. Hillaire-Marcel, U-Th constraints on the duration of Heinrich events H0 to H4 in southeastern Labrador Sea, *Paleoceanography*, under revision.

Vaughn, D. G., and C. S. M. Doake, Recent atmospheric warming and retreat of ice shelves on the Antarctic Peninsula, *Nature, 379*, 328-331, 1996.

Verbitsky. M., and B. Saltzman, A diagnostic analysis of Heinrich glacial surge events, *Paleoceanography, 10*, 59-66, 1995.

Weaver, A. J., Millenial timescale variability in ocean/climate models, this volume.

Weertman, J., Mechanism for the formation of inner moraines found near the edge of cold ice caps and ice sheets, *J. Glaciol., 3*(30), 965-978, 1961.

Wright, H. E., Tunnel values, glacial surges and subglacial hydrology of the Superior Lobe, Minnesota, in *The Wisconsinan Stage*, edited by R. F. Black, R. P. Goldthwait, and H. B. Williams, Geol. Soc. Am. Memoir 36, 251-276, 1973.

Wu, G.-P., and C. Hillaire-Marcel, AMS radiocarbon stratigraphies in deep Labrador Sea cores: paleoceanographic implications, *Can. J. Earth Sci. 31*, 38-47, 1994a.

Wu, G.-P., and C. Hillaire-Marcel, Oxygen isotope compositions of sinistral Neogloboquadrina pachyderma tests in surface sediments: North Atlantic Ocean, *Geochim. Cosmochim. Acta, 58*, 1303-1312, 1994b.

Yuen, D. A., and G. Schubert, The role of shear heating in the dynamics of large ice masses, *J. Glaciol. 24*(90), 195-212, 1979.

G. K. C. Clarke and S. J. Marshall, Department of Earth and Ocean Sciences, 2219 Main Mall, University of British Columbia, Vancouver, B.C., V6T 1Z4, Canada. (e-mail: clarke@eos.ubc.ca; marshall@eos.ubc.ca)

C. Hillaire-Marcel, G. Bilodeau, C. Veiga-Pires, GEOTOP, Université du Québec à Montréal, Montréal, Québec, H3C 3P8, Canada. (e-mail: chm@uqam.ca)